Acoustic emission from pitting corrosion in stressed stainless steel plate

C. K. Lee[1], J. J. Scholey[2], S. E. Worthington[3], P. D. Wilcox*[1], M. R. Wisnom[2], M. I. Friswell[2] and B. W. Drinkwater[1]

The acoustic emission (AE) technique is used to detect and study the AE signals emitted from pitting corrosion on 316L stainless steel plate samples subjected to different levels of surface stress. The tests are performed in a four point bend using accelerated localised salt water corrosion driven by a potentiostat. The AE event rate and the corrosion rate are both found to be affected by the different surface stresses on the plate. After an initial stress dependent phase that lasts around two hours, the AE event rate reduces to a fairly steady rate that is independent of the applied stress. The statistics of the AE data collected from pitting in these specimens is used as the input into a model of an AE corrosion detection system in a larger scale structure. Such a model can be used to estimate the performance of the system as a function of parameters such as threshold level and sensor separation.

Keywords: Acoustic emission, Corrosion, Pitting, Probability of detection, False call ratio

Introduction

Acoustic emission (AE) testing is a well known technique for detecting defects such as fatigue cracks[1] and stress corrosion cracking[2] in structural components. Acoustic emission is generated by a rapid release of energy within a material and propagates through a structure as a transient elastic wave. The basis of AE testing is to detect these elastic waves using sensitive transducers attached on the surface of the structure.

In a typical commercial AE system used to monitor an industrial component,[3] signals are recorded from multiple sensors and when the amplitude of signals satisfies a predefined threshold criterion, the system records what is termed an AE 'hit'. The time delay between hits on various sensors may be used for triangulation to estimate the location of the event that caused the hit. Various empirical parameters may be extracted from the waveform causing a hit, including maximum amplitude, energy, rise time, etc. The cumulative number (count) and intensity of AE hits may also be considered.[4] The overall goal is to use the AE system to detect, locate and quantify damage. Acoustic emission for structural health monitoring (SHM) has been widely used[5] to monitor, for example, industrial oil tanks,[6] pressure vessels[7] and aircraft.[8]

Pitting corrosion has been the subject of numerous electrochemical studies. In this work a standard electrochemical potentiostat circuit was used. Pitting corrosion was induced in stainless steel working electrodes stressed in four point bend by isopotential polarisation to 500 mV_{SCE} (standard calomel electrode), i.e above the pitting breakdown potential E_p, which was determined to be 400 mV_{SCE} in 1000 ppm Cl.

Rettig and Felsen[9] applied the AE technique to the problem of corrosion detection and initiated some work in correlating acoustic emission with corrosion processes. Methods were developed to follow corrosion reactions and to monitor the corrosion of actual structures. A difference in AE activity was observed for a metal immersed in various different corrosive liquids. This work clearly showed that the AE technique could be used to detect corrosion processes.

The correlation of acoustic activity with the rate of corrosion in mild steel using dilute hydrochloric acid was investigated by Seah *et al.*[10] It was shown to be possible to detect different stages of corrosion (mainly uniform corrosion, non-uniform corrosion and intense localised corrosion) based on the observed AE count rate. The corrosion rate was increased by using more concentrated hydrochloric acid which in turn caused an increase in AE events. The correlation between the AE count and corrosion rate was presented and the results showed that a higher AE count was detected with higher corrosion rate.

A good correlation between AE activity and pitting damage on austenitic stainless steel in acidified saline solution was also found by Mazille *et al.*[11] The corrosion rate was controlled by a potentiostat whereby an increase in the applied anodic current density of the potentiostat increased the corrosion rate and the number of pits on the stainless steel plate. Again, the results showed that the total number of recorded AE events was

[1]Department of Mechanical Engineering, University of Bristol, BS8 1TR, UK
[2]Department of Aerospace Engineering, University of Bristol, BS8 1TR, UK
[3]Nexia Solutions, Materials Group, B170, Sellafield Works, Cumbria, CA201PG, UK

*Corresponding author, email p.wilcox@bris.ac.uk

© 2008 Institute of Materials, Minerals and Mining
Published by Maney on behalf of the Institute
Received 14 August 2007; accepted 21 October 2007
DOI 10.1179/17432780 8X286176

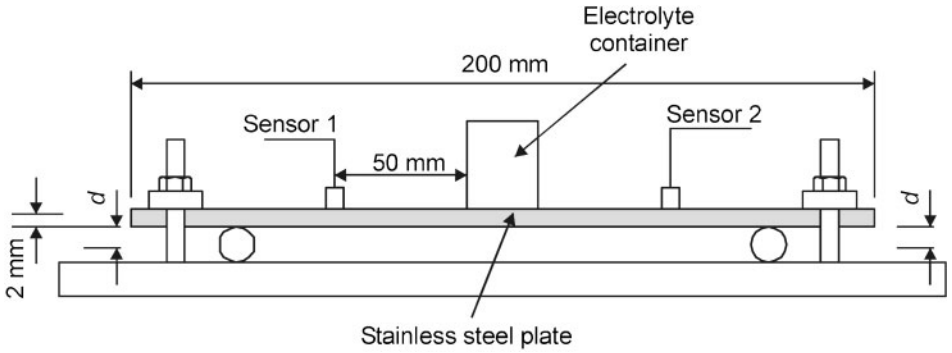

1 Experimental apparatus

in good correlation with the applied polarisation potential.

Cakir *et al.*[12] measured the AE signals from a rectangular bar of 316L stainless steel during slow rate tensile testing at a constant strain rate in a corrosive solvent. It was found that no AE was detected if the polarisation potential of the potentiostat was below the pitting potential even though a plastic deformation beyond necking of the sample was obtained. Acoustic emission activity was only detected if the polarisation potential was increased above the pitting potential. The increase in polarisation potential above pitting potential accompanied by the increase in AE activity indicates a close correlation between pitting corrosion and AE events. When the polarisation potential was held above the pitting potential, a burst of AE signals was detected at an early stage of homogeneous plastic deformation of the specimen during tension. Although there was an increase in the AE activity, the amplitude of the AE signals remained unchanged. This sudden increase in AE signals during plastic deformation was speculated to be due to the rupturing of caps of corrosion product that form over corrosion pits.

Fregonese *et al.*[13] used the AE technique to study the development of pitting corrosion on AISI 316L austenitic stainless steel. Using different polarisation potentials at different intervals, the initiation and the propagation stages of the pit formation was studied separately. Low levels of AE activity were recorded during initiation of the pits but the level increased during the propagation stage.

The literature shows the development of the AE technique for corrosion monitoring, including some work performed on pitting corrosion in stainless steel. Previous work has correlated AE activity with corrosion rate under varying conditions. The aim of the present paper is to provide a quantitative investigation into the AE signals from localised pitting corrosion on the surface of a stainless steel plate under stress and to show how this data may be used as the input to a quantitative model of a complete AE system for corrosion detection.

The first part of the present paper examines the AE signals emitted from corrosion of stainless steel plate samples subjected to different surface stresses levels, introduced through bending. The studies provide an understanding of the effect of surface stresses on the AE from pitting corrosion, the corrosion rate and the resulting surface morphology of the corroded area. The results from this study are used to estimate statistical parameters of AE from the pitting corrosion process.

Of course it is relatively easy to obtain AE data from corrosion using small samples in a laboratory environment. However, in order to use AE testing to detect corrosion in a real structure, it is necessary to understand how parameters such as background noise level, threshold level and intersensor affect performance. Before this can be attempted it is also necessary to decide how the performance of an AE system should be quantified, the challenge being the stochastic nature of AE events and their locations. Olin and Meeker[14] highlighted a collection of statistical models that could be applied to non-destructive evaluation (NDE) using ultrasonic and eddy current methods, but there is currently no equivalent for AE. In the second part of the paper, the framework of a statistical model of the AE process is proposed that uses the concepts of probability of detection (POD) and false call ratio (FCR) as performance metrics. The model uses an analytical model to simulate wave propagation in a larger structure and combines this with the earlier experimental data to estimate the POD. The statistical properties of background noise events in an uncorroded control sample were also experimentally measured and used to estimate the FCR. It is then shown how it is possible to estimate the dependence of POD and FCR in a real structure as a function of parameters such as spacing between sensors and threshold level.

Experimental

Specimen preparation

Stainless steel 316L plates with dimensions of $200 \times 37{\cdot}5 \times 2$ mm were used in the study. No surface preparation other than cleaning with acetone was performed on the plate, as the intention was to induce corrosion on the normal manufactured surface to represent a real industrial component.

Control of stress level and corrosion rate

A fixture as shown in Fig. 1 was built to bend the plate using a four point bend configuration. The nuts were adjusted to deflect the ends of the plate by different distances d, so that different tensile surface stresses were produced on the top surface of the central region of the plate. A cylindrical tube, approximately 18 mm in diameter was placed in the centre of the plate and the base was sealed to the plate with silicon gel to form a watertight container. Saturated sodium chloride solution was poured into the container and the corrosion process was driven using a potentiostat (Gill AC potentiostat, manufactured by ACM Instruments,

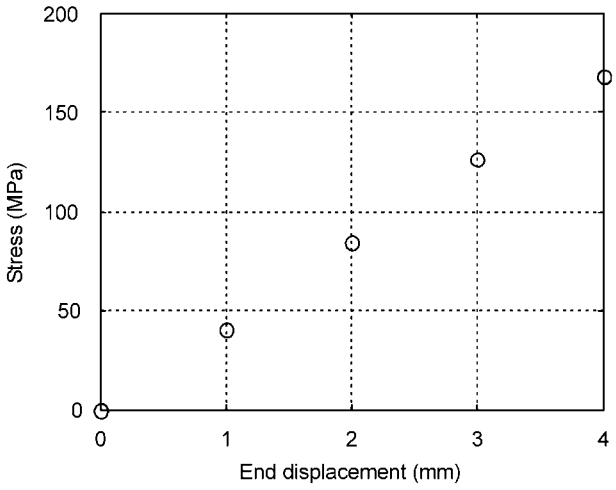

2 Surface stress calculated from strain gauge readings for different end displacements

Cark, UK). The specimen was connected as the working electrode, platinum wire was used as the auxiliary electrode and saturated calomel as the reference electrode. The auxiliary and reference electrodes were placed in the salt water solution.

Surface stress measurement

Initial work using a strain gauge to determine the surface strain in the centre of the plate for different end displacements, d, was performed. The surface stresses were calculated using a Young's modulus of 193 GPa[15] and the results for different deflection distances are shown in Fig 2.

Acoustic emission setup

A commercial AE system (model PCI2 manufactured by the Physical Acoustic Corporation, Princeton Jct, NJ, USA) was used for AE measurements. The sensors used were custom made, non-resonant devices containing a 3 mm diameter, 3 mm thick piezoelectric disc (made from Pz27 material manufactured by Ferroperm Piezoceramics, Storrington, UK). By intentionally operating below their first resonant frequency, these sensors can be used to provide a fairly flat frequency response between 50 and 600 kHz. This enables them to provide a high fidelity measurement of the surface displacement being measured that is not contaminated by the properties of the sensor. Two of these sensors were bonded using superglue 50 mm away from the centre of the plate on either side of the electrolyte container as shown in Fig. 1. The sensors were calibrated *in situ* using a laser interferometer to determine their response to out of plane surface displacement on the samples used for the tests described in this paper. The calibration curve exhibits a small amount of frequency dependence but is of the order of $3{\cdot}48 \times 10^{-9}$ m V^{-1}. The AE signals from each sensor were pre-amplified with a gain of 40 dB and no filtering was used. The threshold of the AE system was set at 32 dBae (the dBae scale is a decibel scale of voltage referenced to 1 μV, hence 32 dBae is approximately equivalent to a surface displacement of $0{\cdot}14 \times 10^{-12}$ m), which was slightly above the background noise level measured at 30 dBae. The AE system was set so that signals were only recorded when hits (i.e. voltages exceeding the threshold value) were detected on both sensors within a 10 μs period of each other. This is referred to as a Δt filter and in theory means that only AE events occurring within a limited portion of the structure are recorded. In this case, the Δt filter corresponds to events within the central 30 mm of the plate, assuming a signal propagation velocity of 3 mm μs^{-1}. The signals were recorded with a pretrigger of ~200 μs so that they encompassed the complete waveform from the AE event. All the subsequent analysis of the recorded waveforms was performed in Matlab (The Mathworks Inc., Natick, MA, USA).

A simple test was conducted to test the AE system parameters by leaving the system running on plate without the corrosion generation equipment operating for a total of 12 h. Over this period no emissions were detected, indicating that the AE system would not be triggered on either background electrical noise or AE events occurring outside of the central area of the plate, such as stick–slip phenomena at the clamping nuts.

Experimental procedure

Five identical plate samples were tested according to the following procedure while being subjected to different levels of bending load. Each plate was weighed before it was placed in the fixture for testing. The nuts were adjusted to obtain a specified surface stress in the centre of the plate and then the electrolyte container was attached. Sodium chloride solution of 2% concentration by mass was poured into the container and the electrodes from the potentiostat were immersed in the salt water 25 mm above the surface of the plate. The polarisation potential was fixed at 500 mV_{SCE} and the AE system was used to monitor the sample over a period of 5 h. After 5 h of corrosion, the potentiostat was removed and the container was refilled with fresh sodium chloride solution. The AE test was then left to run for around 15 h. After the test, the container and silicon gel were removed from the surface of the plate and the plate was reweighed to determine the amount of weight loss.

Results and discussion

AE events

Typical time domain signals recorded from both sensors corresponding to a single AE event are shown in Fig. 3*a*. The threshold level and arrival time difference (Δt) are labelled on the signals. The peak amplitude values indicated are automatically extracted in Matlab and these are used for subsequent post-processing.

Figure 4 shows the AE event amplitudes as a function of time for three plates with different surface stresses of 0, 40·3, 84·1, 126·4 and 167·9 MPa. The AE event at the beginning with an amplitude of around 100 dBae corresponds to a pencil lead break on the plate surface that was performed to check whether the sensors were working. For all stress levels, AE events were detected during the 5 h period when the potentiostat was switched on. It was observed that, over this period, the amplitude of the AE signals remained relatively constant between 33 and 45 dBae. After the potentiostat was switched off, it was found that a negligible number of AE signals were detected.

In order to investigate the frequency content of the AE signals, each signal was Fourier transformed in Matlab to obtain its frequency spectrum. Examples are shown in Fig. 3*b*. The frequency of the peak amplitude

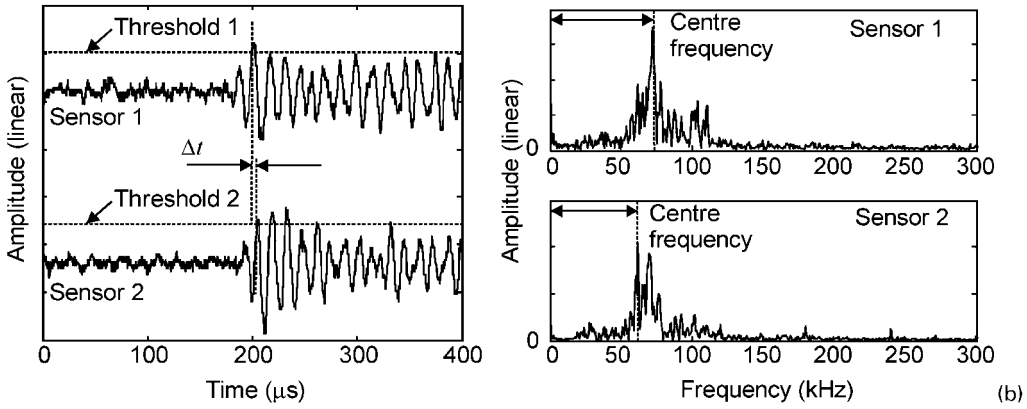

3 ***a*** **pair of typical time domain AE signals from each sensor for same event and** ***b*** **corresponding frequency spectra of AE signals**

of the frequency spectrum was then automatically extracted to provide an indication of the dominant frequency present in the signal. For brevity the dominant frequency calculated in this manner will subsequently be referred to as the frequency of an event. Figure 5 shows the frequency of the AE events as a function of time for the five plates at the five different surface stresses. There is a large amount of scatter on these results, but the majority of events have dominant frequencies below 200 kHz. However, the maximum frequency of any event increases from below 60 Hz at 0 MPa to over 400 Hz at stresses above 125 MPa.

Figures 4 and 5 qualitatively suggest that the amplitude of the AE events is independent of stress level, although it is clear that higher stress levels generate a larger number of events. To examine this further, the time evolution of the cumulative number of AE events recorded for different stress values was analysed as shown in Fig. 6. Particularly for the higher stress levels, the curves exhibit a distinctive bend where two periods of fairly steady low AE activity are separated by a short period where the rate is much higher. The initial low rate of events probably reflects the pitting incubation time when the local breakdown of the passive film is occurring. The rapid increase in events is presumed to reflect the period when a significant number of new pits are forming and the subsequent reduction in the event rate indicates that the formation of new pit sites has slowed. This can be either due to a stable pitting regime having been established with well defined anodic and cathodic regions, or due to the effective depassivation of the surface leading to general corrosion in an acidified chloride solution when the pit mouths are breached and the contents leak out.

To examine this further, Fig. 7*a* shows the average rate of AE events over the first two hours of the test period plotted against the surface stress level. It can be seen here that the correlation is almost linear. However, the rate of AE events averaged over the period from 2 to 5 h is relatively constant as shown in Fig. 7*b*. The overall average corrosion rate in kilograms per second was calculated for each sample using the weights

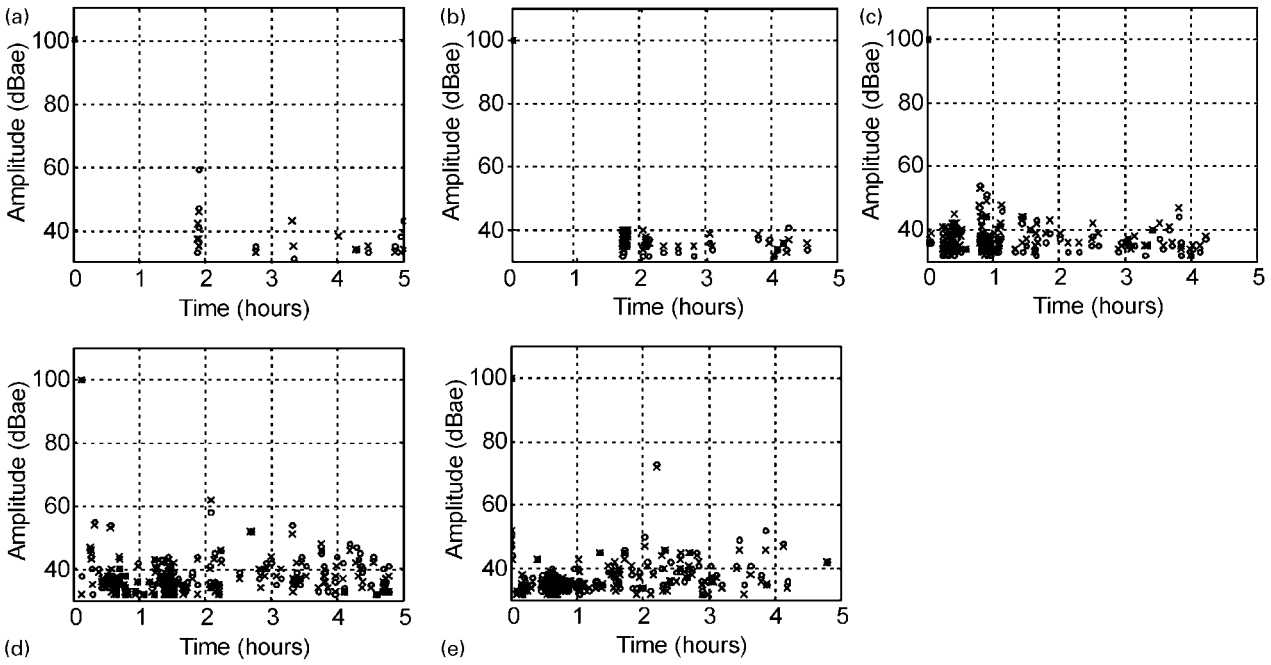

a 0 MPa; *b* 40·3 MPa; *c* 84·1 MPa; *d* 126·4 MPa; *e* 167·9 MPa

4 Acoustic emission signals detected during pitting using potentiostat showing amplitude of signal from sensor 1 (cross) and sensor 2 (open circles) for surface stresses

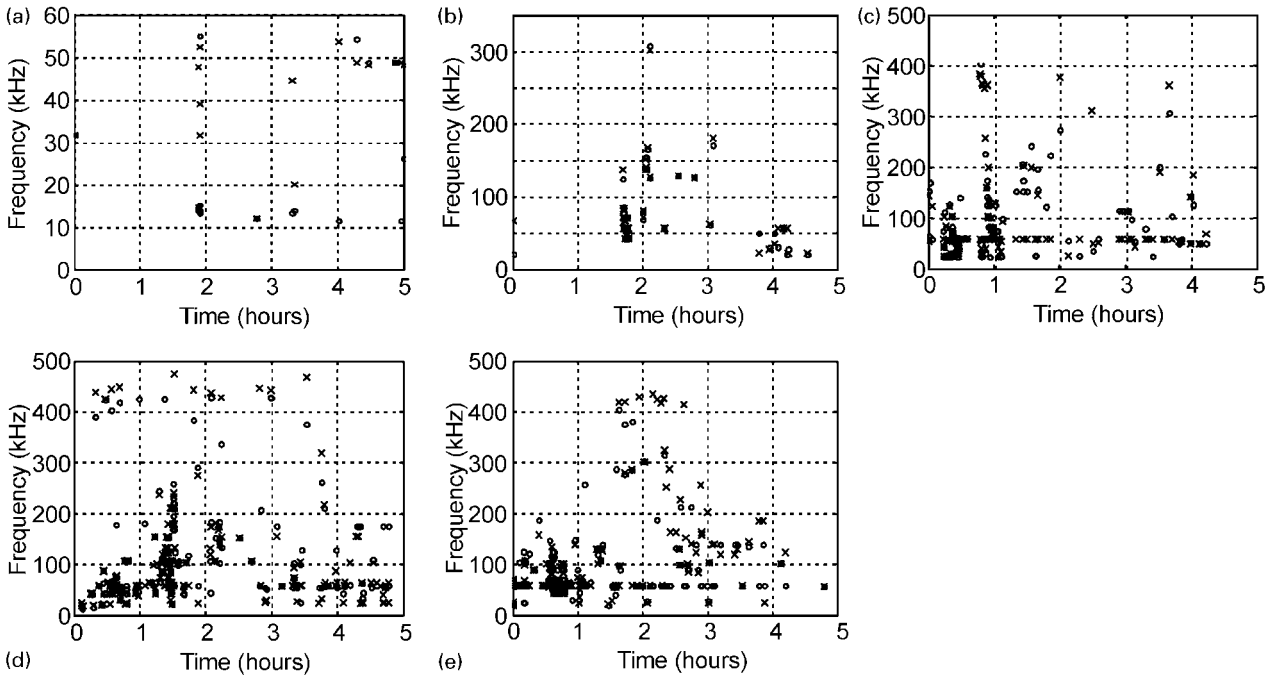

a 0 MPa; *b* 40·3 MPa; *c* 84·1 MPa; *d* 126·4 MPa; *e* 167·9 MPa

5 Frequency spectra of detected AE signals from sensor 1 (cross) and sensor 2 (open circles) for surface stresses

recorded before and after the test. For samples where the full surface showed general attack by acidified pit solution, it was found that overall average corrosion rate increased almost linearly with respect to the surface stress as shown in Fig. 8. However, specimens which maintained localised pitting showed weight loss below this line. This indicates that in acidified chloride solutions at least, general corrosion of stainless steel is proportional to the surface stress.

Acoustic emission event amplitude and frequency distribution

The amplitude distribution of the signals for each stressed plate was investigated. Figure 9 shows the AE

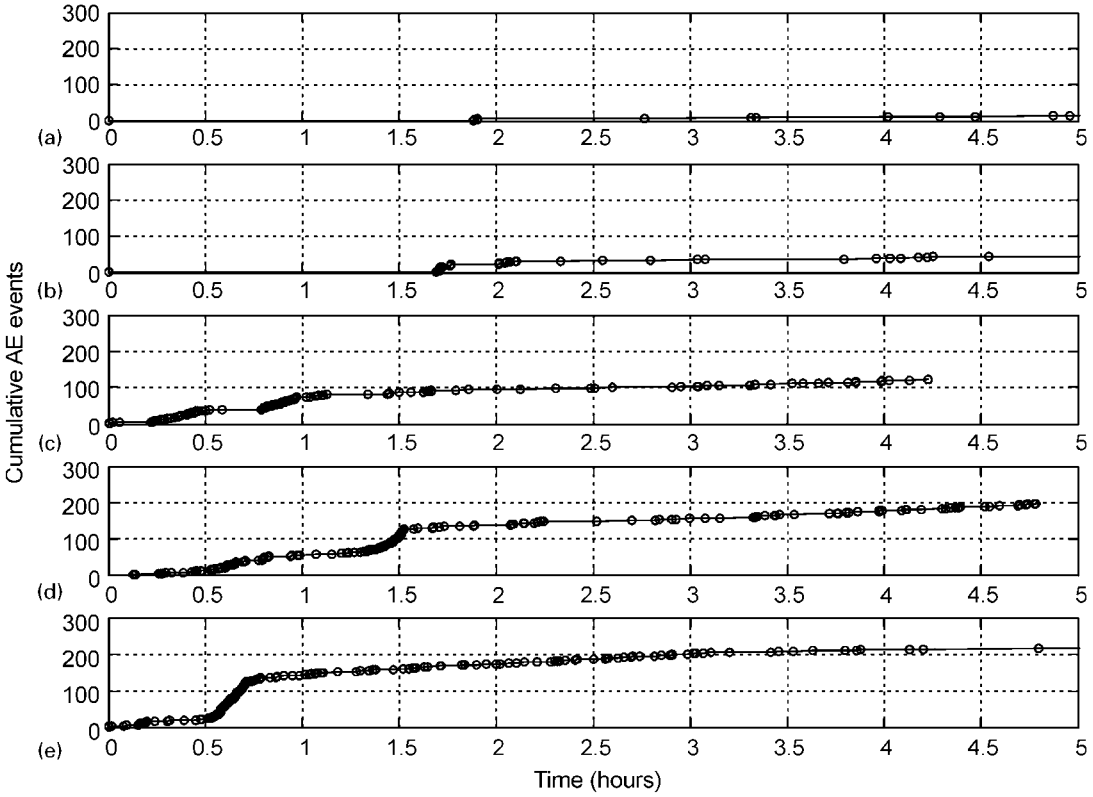

a 0 MPa; *b* 40·3 MPa; *c* 84·1 MPa; *d* 126·4 MPa; *e* 167·9 MPa

6 Cumulative AE events for different stresses

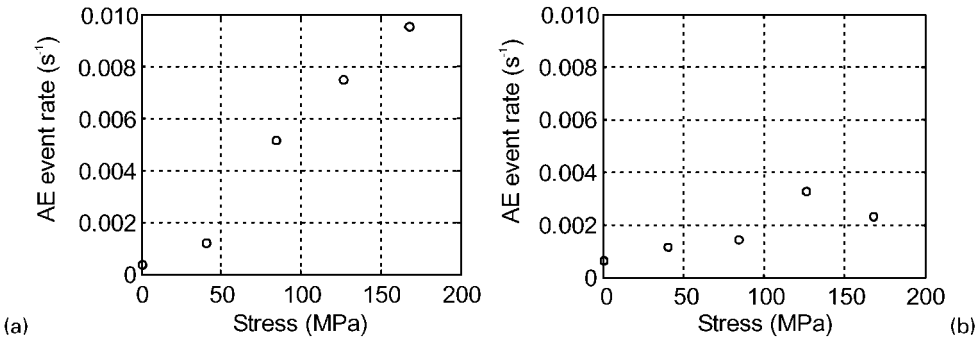

7 Acoustic emission event rate for plate versus surface stress obtained by *a* averaging over first two hours and *b* averaging over period from 2 to 5 h

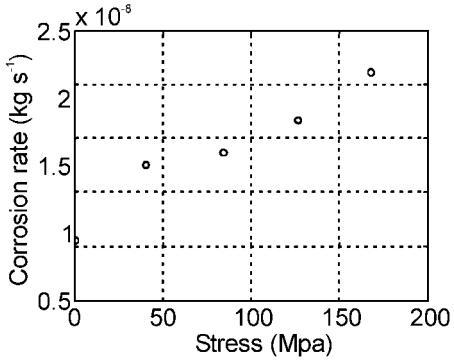

8 Overall average corrosion rate versus surface stress

event rate as a function of event amplitude for the five differently stressed plate samples. The graphs show the rates obtained by averaging over the 0–2 h and 2–5 h periods. Although there was an increase in the AE event rate for the differently stressed plate over the 0–2 h period of corrosion (*see* Fig. 7), the shape of the amplitude distribution of AE events from different stresses level remains approximately constant. The shape is approximately Gaussian with a mean amplitude between 33 and 36 dBae. This effect of a unchanged amplitude of the AE signals even with an increase in AE activity was also mentioned by Cakir *et al.*[12] In the second part of the present paper, the results from the hit amplitude distribution for differently stressed plates are used to compute the probability of detection for corrosion detection using different sensor configurations. The distribution of the frequency of the AE events was also analysed as shown in Fig. 10. Here there is no clear distribution evident although the majority of events lie within in the broad range of 20–200 kHz. It is noted that at high stress levels more high frequency events are recorded. The reason for this is unclear but may relate to the unsustained initiation of stress corrosion cracking.

Surface morphology

Photographs of the surfaces of the corroded area of the plates are shown in Fig. 11. The pits obtained from the plate without stress are wide and shallow. It can be seen

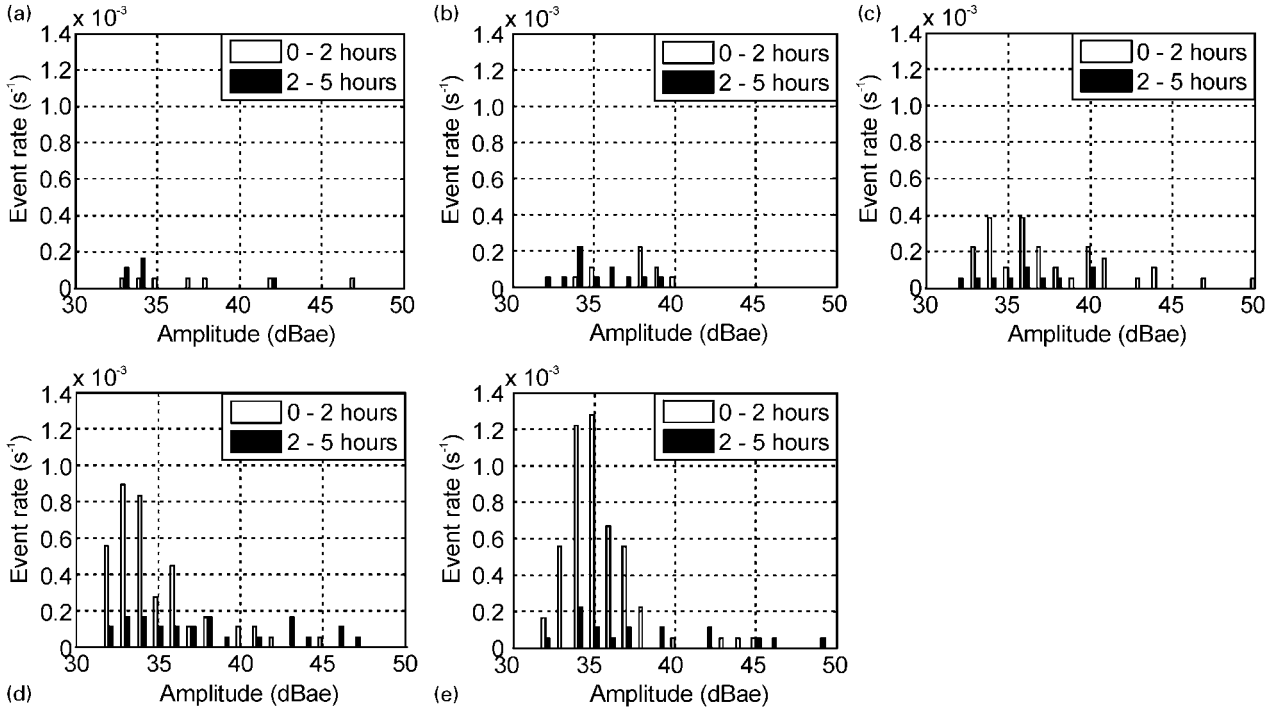

a 0 MPa; *b* 40·3 MPa; *c* 84·1 MPa; *d* 126·4 MPa; *e* 167·9 MPa

9 Event rate amplitude distributions obtained by averaging over 0–2 h and 2–5 h for different stresses

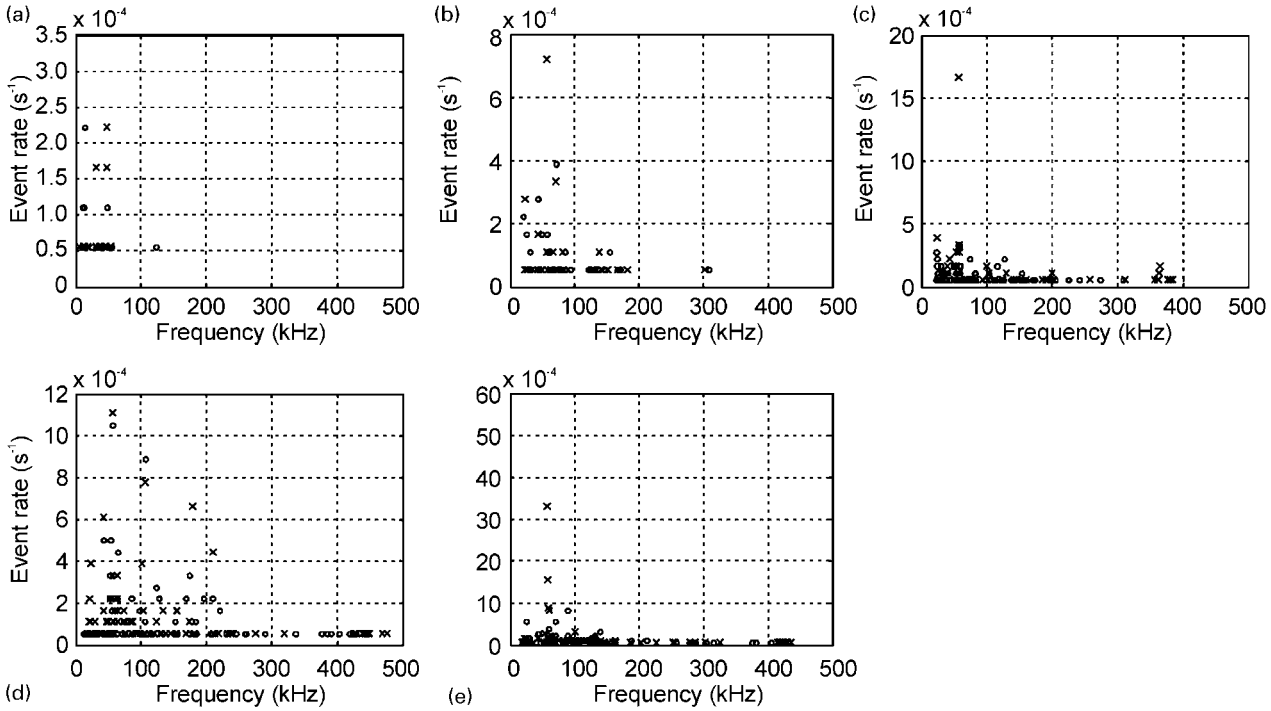

a 0 MPa; *b* 40·3 MPa; *c* 84·1 MPa; *d* 126·4 MPa; *e* 167·9 MPa

10 Event rate frequency distributions for sensor 1 (cross) and sensor 2 (open circles) obtained by averaging over 0–2 h and 2–5 h for different stresses

that more pits are formed on the more highly stressed plates and visual inspection indicated that the depth of the pits was deeper.

The increases in AE event rate, corrosion rate and number of pits with respect to the stresses in the plate can be explained as follows. Pitting will initiate at discontinuities in the passive oxide. In the unstressed state these would be at inclusions such as MnS or other foci of low passivity such as microcrevices. In the highly stressed state more foci for pit initiation are clearly generated. It is likely that in some areas of marginal passivity such as grain boundaries the stress is sufficient to fracture the oxide film and repassivation may not be fully effective due to localised chromium depletion. At lower stresses fewer pits tend to develop as there are fewer competing sites. If the pits break open, the viscous acidified chloride pit solution tends to remain at the surface and overall depassivation and corrosion of the

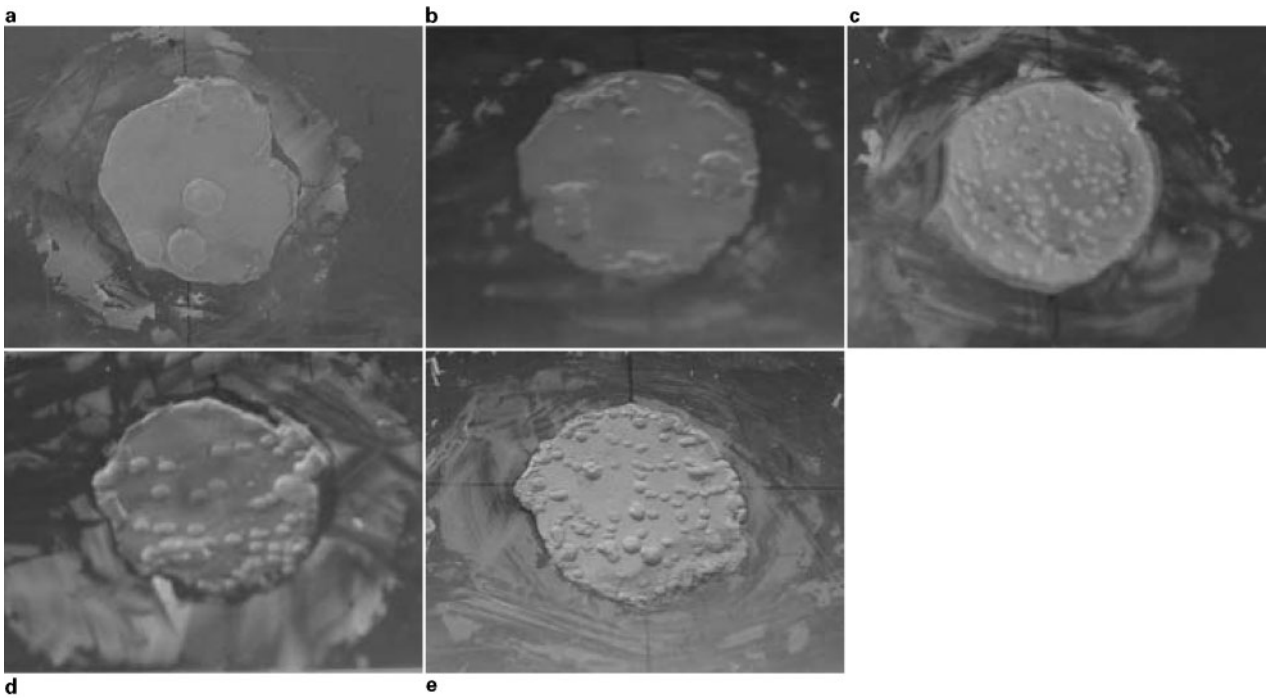

a 0 MPa; *b* 40·3 MPa; *c* 84·1 MPa; *d* 126·4 MPa; *e* 167·9 MPa

11 Photographs of corroded areas for samples subjected to different surface stresses

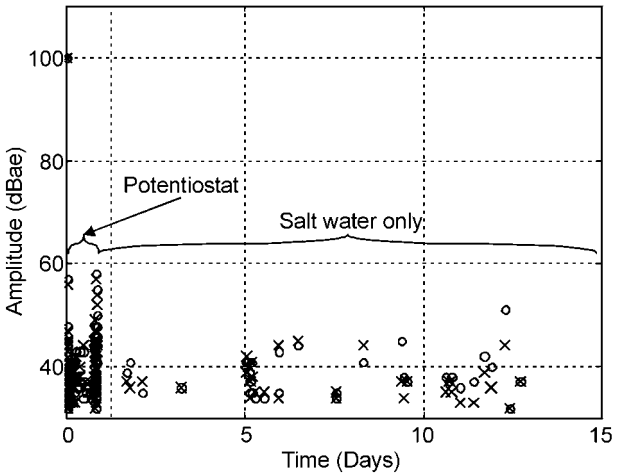

12 Acoustic emission signals detected by sensor 1 (cross) and sensor 2 (open circles) on stressed plate with initial period of potentiostat driven corrosion followed by longer period of salt water corrosion

surface was seen on many of the specimens as a consequence.

The mechanism of the AE signals from pitting has yet to be fully explained. Some articles in the literature[10,12,13] mention that the inside of the pits may promote hydrolysis reactions and that the subsequent release of hydrogen is the source of the AE signals. This hypothesis has yet to be confirmed by complementary tests.

Acoustic emission events from salt water corrosion

It was noted previously that no AE could be detected from a stressed plate sample immersed in salt water, unless the corrosion process was driven using a potentiostat. Given the observation that there are two stages to the corrosion process it was decided to investigate whether AE could be detected without a potentiostat at the second stage after the corrosion process had been initiated. A plate sample was bent to produce a stress of 168 MPa in the centre of the plate. The initial corrosion on the plate was achieved using a potentiostat. The potentiostat was then removed and the salt water was replaced. The experiment was left untouched for a total of 13 days. The results in Fig. 12 show that AE events were recorded during salt water corrosion throughout the 13 days of the test. Although the occurrence of the AE events was infrequent, the amplitude distribution of the hit signals is similar to those obtained from earlier experiments. This suggests that the potentiostat is required to initiate the corrosion process by breaking down the passive layer. However, once the passive layer is penetrated the corrosion process will continue without the potentiostat, albeit at a lower rate than if one is used.

Estimating performance of AE for corrosion detection

The purpose of this part of the paper is to demonstrate how the experimental data from the coupon samples described previously can be used to estimate two performance metrics of an AE corrosion detection system on a real structure. The following performance metrics are widely used to describe the performance of various non-destructive evaluation (NDE) techniques[14] in the context of tests applied to populations of components:

(i) POD: the fraction of genuinely defective samples that are correctly classed as defective, i.e. the true positive fraction

(ii) FCR: the fraction of pristine samples that are incorrectly classified as defective, i.e. the false positive fraction.

These metrics are based on populations of components and are not directly applicable to the corrosion detection system that is likely to be permanently installed on a single structure. Instead the following modifications are proposed:

(i) POD: the probability that a genuine AE event due to corrosion will be detected

(ii) FCR: the fraction of spurious events estimated to occur that are incorrectly interpreted as being due to corrosion.

This definition of FCR is arguably somewhat artificial since the total number of spurious events could be unlimited if there is no constraint on the minimum amplitude. However, it is sufficient for the purposes of this demonstration where a Gaussian fit to measured data allows a finite estimate to be made.

The ideal situation for any test is a POD of 100% and a FCR of 0%. The reality is that one or both of these ideals must be compromised, and the use of such metrics enables the effect of changing test parameters, such as sensor spacing, to be quantified. The approach proposed here is to obtain statistical models of the amplitude distribution of AE events due to both background noise and the corrosion process itself. In both cases, it is assumed for simplicity that the amplitude distribution in dBae is Gaussian (i.e. the actual amplitude distribution is log normal). In practice, the background noise distribution must be measured *in situ* and under normal plant operating conditions for each application. The reason for fitting distributions to the experimentally measured corrosion and noise data is that it enables the total rate of corrosion and noise events to be estimated by extrapolation of the curves and integration. If this was not performed, absolute values of event and noise rates could be obtained directly from experimental data, but these could not be converted to probabilities.

Measurement of noise amplitude distribution

The PAC system AE was used to detect the noise amplitude distribution in the same lab where the corrosion tests were performed. To do this, the same sensor configuration (*see* Fig. 1) was used on a narrow plate specimen. The threshold level of the AE system was set to the relatively low value of 10 dBae and data were recorded over a 2 h period. The measured amplitude distribution is shown in Fig. 13*a*. A Gaussian curve was fitted to the amplitude distribution of the noise by iteratively adjusting the amplitude, mean and standard deviation values to minimise the cumulative least squares deviation with the experimental points.

Measurement of signal amplitude distribution

As an example of corrosion data, the amplitude distribution obtained from the coupon stressed to 167·9 MPa is used. This amplitude distribution is shown in Fig. 13*b* and has a cut-off point at 32 dBae at the

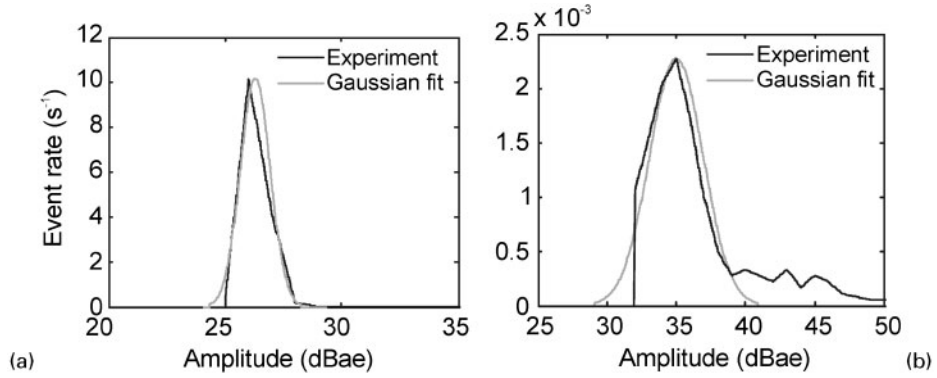

13 Gaussian best fit curves for *a* noise and *b* corrosion AE events

fixed threshold level. A Gaussian curve is again fitted to the available data above 32 dBae using the same procedure as for the noise distribution. It is noted that this fit is not altogether satisfactory for the higher amplitude events.

Calculation of POD and FCR

Once the noise and signal amplitude distributions have been determined, the POD and FCR may be calculated, in the first instance, as a function of threshold level

$$POD(t) = \frac{\int_{t}^{\infty} G(a)\mathrm{d}a}{\int_{-\infty}^{\infty} G(a)\mathrm{d}a}$$
$$PCR(t) = \frac{\int_{t}^{\infty} N(a)\mathrm{d}a}{\int_{-\infty}^{\infty} N(a)\mathrm{d}a} \quad (1)$$

where a is the amplitude in dBae, $G(a)$ is the amplitude distribution of signals from corrosion, $N(a)$ is the amplitude distribution of noise signals and t is the threshold level (in dBae). Figure 14*a* graphically demonstrates the POD calculation.

The POD and FCR can be plotted as a function of threshold level t, leading to the characteristic curves shown on the graph in Fig. 14*b*. The ideal situation for a test is where the curved parts of the POD and FCR occupy non-overlapping regions of t. This means that a threshold can be chosen between the two where the FCR is close to 0 and the POD is close to 100%. Form the data in Fig. 14 it can be seen that this is very nearly the case for threshold levels of around 28–30 dBae. This is of course to be expected, because the data were taken from small samples in a laboratory environment with sensors in close proximity to the corrosion source. The next section describes how the same data may be used to investigate the performance of corrosion detection on a larger structure.

Estimating the performance of corrosion detection system

As an example of the way in which the POD and FCR data can be used, the effect of sensor separation is considered. Because the experimental samples are plate-like, the AE signals from a source decay in inverse proportion to the square root of propagation distance from the source.[16] This means that the amplitude data from the small samples can be adjusted to investigate the effect of distance between source and sensor and the POD curve recalculated. Figure 15 shows the POD curves for different distances between the source and sensor. As the distance between the source and sensor increases, the amplitude of the AE signals decreases and therefore the POD curve shifts towards the FCR curve. This means that it is no longer possible to choose a threshold level that gives 100% POD and 0% FCR, and instead a compromise must be made.

Conclusions

Experiments have been performed to investigate the AE from salt water pitting corrosion in stainless steel plates subjected to varying levels of bending stress, with the corrosion accelerated using a potentiostat. In the pitting initiation stage, the AE event rate has been found to be approximately proportional to the level of tensile surface stress on the sample. After this, the AE event rate and becomes largely independent of the stress level. The overall general corrosion rate if the surface is

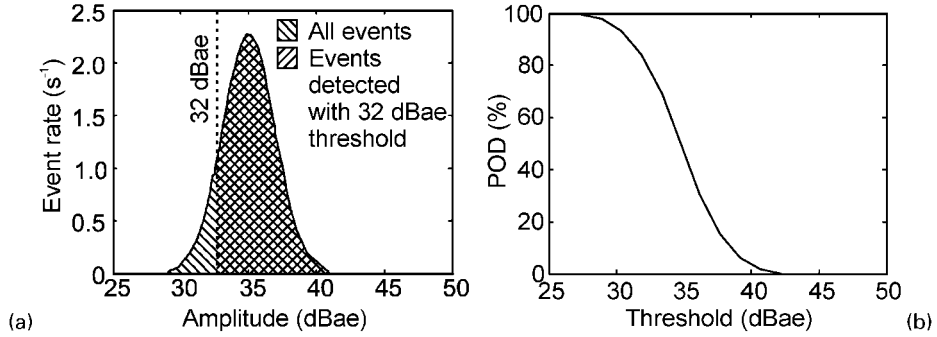

14 *a* schematic illustration of POD calculation and *b* resulting graph of POD versus threshold level

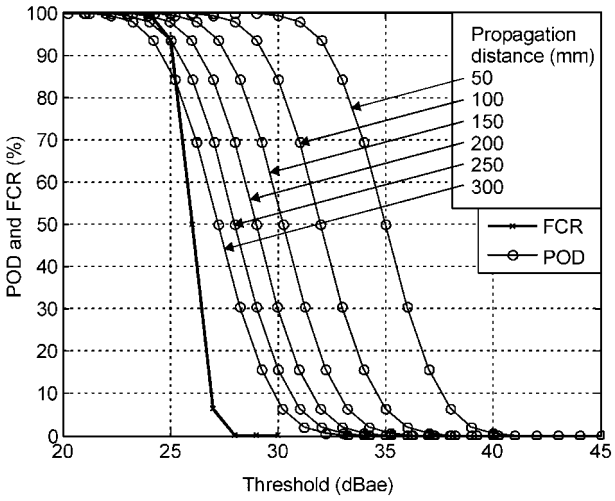

15 Probability of detection and false call ratio curves as function of threshold level for different propagation distances

depassivated has also been found to be approximately proportional to the level of tensile stress in the sample. Although the potentiostat is needed to initiate corrosion, it has been found that once initiated, corrosion and AE will continue at a low rate without the potentiostat. An interesting observation of practical significance is that the amplitude distribution of AE events from corrosion seems to be independent of both the stress level and whether the potentiostat is used; the AE parameter that varies most with the corrosion process is the rate of AE events. The paper has also shown how the data from small coupon tests may be used to estimate the performance of an AE system to detect corrosion in real plant or components.

Acknowledgements

This work was supported by EPSRC funded Research Centre in NDE (RCNDE) targeted research programme (grant no. GR/T01136/01), Nexia Solutions, Airbus and Rolls-Royce. The stainless steel samples were supplied by Nexia Solutions.

References

1. C. M. Scala and S. M. Cousland: *Mater. Sci. Eng.*, 1983, **61**, (3), 211–218.
2. R. B. Clough, J. C. Chang and J. P. Travis: *Scr. Metall.*, 1981, **15**, (4), 417–422.
3. C. B. Scruby: *J. Phys. E, Sci. Instrum.*, 1987, **20**, (8), 947–953.
4. A. Berkovits and D. N. Fang: *Eng. Fracture Mechan.*, 1995, **51**, (3), 401–409.
5. D. O. Harris and H. L. Dunegan: *Non-Destruct. Test.*, 1974, **7**, (3), 137–144.
6. K. L. Komarov, A. N. Ser'eznov, V. V. Murav'ev, L. N. Stepanova, E. Y. Lebedev, S. I. Kabanov and M. V. Gerashchenko: *Russ.. J. Nondestruct. Test.*, 2001, **37**, (3), 232–237.
7. C. B. Scruby and H. N. G. Wadley: *Prog. Nucl. Energ.*, 1983, **11**, (3), 275–297.
8. J. M. Carlyle: *NDT Int.*, 1989, **22**, (2), 67–73.
9. T. W. Rettig and M. J. Felsen: *Corrosion*, 1976, **32**, (4), 121–126.
10. K. H. W. Seah, K. B. Lim, C. H. Chew and S. H. Teoh: *Corros. Sci.*, 1993, **34**, (10), 1707–1713.
11. H. Mazille, R. Rothea and C. Tronel: *Corros. Sci.*, 1995, **37**, (9), 1365–1375.
12. A. Cakir, S. Tuncell and A. Aydin: *Corros. Sci.*, 1999, **41**, (6), 1175–1183.
13. M. Fregonese, H. Idrissi, H. Mazille, L. Renaud and Y. Cetre: *Corros. Sci.*, 2001, **43**, (4), 627–641.
14. B. D. Olin and W. Q. Meeker: *Technometrics*, 1996, **38**, (2), 95–112.
15. F. Pernot and R. Rogier: *J. Matls. Sci.*, 1993, **28**, (24), 6676–6682.
16. P. D. Wilcox, C. K. Lee, J. J. Scholey, M. I., Friswell, M. R. Wisnom and B. W. Drinkwater: Proc. SPIE 2006: smart structures and integrated systems, (ed. Y. Matsuzaki), Vol. 6173; 2006, Bellingham, WA, SPIE.